

# Mid-IR emission of galaxies in the Virgo cluster: II. Integrated properties.\*

A. Boselli<sup>1</sup>, J. Lequeux<sup>2</sup>, M. Sauvage<sup>3</sup>, O. Boulade<sup>3</sup>, F. Boulanger<sup>4</sup>, D. Cesarsky<sup>4</sup>, C. Dupraz<sup>5</sup>, S. Madden<sup>3</sup>, F. Viallefond<sup>2</sup>, and L. Vigroux<sup>3</sup>

<sup>1</sup> Laboratoire d'Astronomie Spatiale, Traverse du Siphon, BP 8, F-13376 Marseille CEDEX 12, France

<sup>2</sup> Observatoire de Paris, 61 Av. de l'Observatoire, F-75014 Paris, France

<sup>3</sup> Service d'Astrophysique, Centre d'Etudes de Saclay, F-91191 Gif sur Yvette, France

<sup>4</sup> Institut d'Astrophysique Spatiale, Bat. 121, Université Paris-Sud, F-91405 Orsay, France

<sup>5</sup> Radioastronomie, Ecole Normale Supérieure, 24 Rue Lhomond, F-75231 Paris CEDEX 05, France

Received , accepted

**Abstract.** We analyse the integrated properties of the Mid-IR emission of a complete, optically selected sample of galaxies in the Virgo cluster observed with the ISO-CAM instrument on board the ISO satellite. The ISO-CAM data allows us to construct the luminosity distribution at 6.75 and 15  $\mu\text{m}$  of galaxies for different morphological classes. These data are used to study the spectral energy distribution of galaxies of different type and luminosity in the wavelength range 2000 Å- 100  $\mu\text{m}$ . The analysis shows that the Mid-IR emission up to 15  $\mu\text{m}$  of optically-selected, normal early-type galaxies (E, S0 and S0a) is dominated by the Rayleigh-Jeans tail of the cold stellar component. The Mid-IR emission of late-type galaxies is instead dominated by the thermal emission from dust. As in the Milky Way, the small dust grains emitting in the Mid-IR have an excess of emission if compared to big grains emitting in the Far-IR. While the Far-IR emission of galaxies increases with the intensity of the interstellar radiation field, their Mid-IR emission is non-linearly related to the UV radiation field. The spectral energy distributions of the target galaxies indicate that there is a linear relationship between the UV radiation field and the Mid-IR emission of galaxies for low or intermediate activities of star formation, while the emission from the hot dust seems to drop for strong UV fields. The Mid-IR colour of late-type galaxies is not related to their activity of star formation.

The properties of the dust emission in the Mid-IR seem more related to the mass than to the morphological type of the target galaxy. Since the activity of star formation is

anticorrelated to the mass of galaxies, this reflects a relationship between the emission of dust in the Mid-IR and the UV radiation field: galaxies with the lowest Mid-IR emission for a given UV field are low mass, dwarf galaxies. These observational evidences are easily explained if the carriers of the Unidentified Infrared Bands that dominate the 6.75  $\mu\text{m}$  emission are destroyed by the intense UV radiation field of dwarf galaxies, although abundance effects can also play a role.

**Key words:** Galaxies: general– Galaxies: ISM– Galaxies: spiral– Infrared: galaxies– Infrared: ISM: continuum

## 1. Introduction

The bulk of the infrared (IR) emission of the interstellar medium (ISM) of galaxies is due to the thermal emission of the dust heated by the interstellar radiation field. Stellar photons are absorbed by the interstellar dust and re-emitted in the IR from  $\sim 4 \mu\text{m}$  to  $\sim 1 \text{mm}$ . The dust emitting in the Far-IR ( $\lambda \gtrsim 70 \mu\text{m}$ ) is probably composed of big grains (with a linear radius  $r \gtrsim 200 \text{Å}$ ) of graphite and silicate in thermal equilibrium with the UV and optical photons of the interstellar radiation field (Désert et al. 1990; Dwek et al. 1997). In the range  $10 \mu\text{m} \lesssim \lambda \lesssim 70 \mu\text{m}$  the emission is usually dominated by very small, three dimensional grains (VSG) mostly composed of graphite ( $10 \text{Å} \lesssim r \lesssim 200 \text{Å}$ ), absorbing mainly in the UV, whose emission is however not negligible also at shorter wavelengths (Désert et al. 1990; Dwek et al. 1997). In the range  $3 \mu\text{m} \lesssim \lambda \lesssim 15 \mu\text{m}$  the emission of the interstellar medium is generally dominated by the Unidentified Infrared Emission Bands (UIB). The carriers of the UIBs and associ-

Send offprint requests to: A. Boselli boselli@astrsp-mrs.fr

\* Based on observations with ISO, an ESA project with instruments founded by ESA member states (especially the PI countries: France, Germany, the Netherlands and the United Kingdom) and with participation of ISAS and NASA

ated continuum, often called Polycyclic Aromatic Hydrocarbons (PAHs) although this assignment is uncertain, are heated stochastically by absorption of single photons and temporarily reach very high temperatures, at which most of the emission occurs (Désert et al. 1990; Dwek et al. 1997).

The knowledge of the dust emission properties of the ISM strongly increased in the last years thanks to the large amount of data obtained by the IRAS satellite, which made an all-sky survey in 4 different filters, at 12, 25, 60 and 100  $\mu\text{m}$ . More recently, the ISO satellite is providing higher quality data in the spectral range  $\sim 3 \mu\text{m} < \lambda < 200 \mu\text{m}$ . In order to analyse the properties of the IR emission of different classes of objects and/or of single galaxies, the ISOCAM and the ISOPHOT consortia constructed a coordinated program of observations of an optically selected, complete sample of late-type galaxies in the Virgo cluster. This sample, which includes a large number of galaxies of different morphological type and luminosity, has been selected to be used as a reference for other studies. Furthermore the sample includes objects in the centre and in the periphery of the cluster in order to study the effects of the environment on the dust emission and on the evolution of galaxies. Because all the selected galaxies are at the same distance, the construction of a reference sample is quite direct.

The selected sample has been observed entirely with CAM and partly with PHOT and LWS. In this paper we report on the integrated properties of the galaxies observed with CAM, thus in the spectral range  $3 \mu\text{m} < \lambda < 20 \mu\text{m}$ . Preliminary results have been already published in Boselli et al. (1997a, Paper I) and Boselli & Lequeux (1997). The data, the analysis of the relationship between the star formation activity and the Mid-IR emission of the few resolved galaxies and the study of the effects of the environment on the properties of the dust emission of late-type galaxies will be discussed in future papers (Boselli et al., in preparation). The purpose of the present paper is to present a reference for other ISOCAM observations. The sample is described in Sect. 2; a brief description of the observations and of the data reduction is given in Sect. 3. In Sect. 4 we analyse the Mid-IR luminosity distribution of the target galaxies, their spectral energy distribution (SED), and the relationships between the Mid- and Far-IR emission of galaxies of different types and luminosities. The discussion and the conclusions are given in Sect. 5.

## 2. The sample

The selected sample is extensively described in Boselli et al. (1997b). Briefly, the sample has been extracted from the Virgo Cluster Catalogue (VCC) of Binggeli et al. (1985) which is complete to  $B_T = 18$  mag. It includes all galaxies with morphological type later than S0, with  $B_T \leq 18$  mag, classified as cluster members by Binggeli et al. (1985; 1993). Because of time limitations, the sample has

been restricted to include only galaxies within a projected distance of 2 degrees from M87, thus belonging to the core of the cluster, and comparison objects in the cluster periphery. The cluster periphery is at an angular distance larger than 4 degrees from the position of the maximum projected galaxy density given by Sandage et al. (1985), but excluding galaxies within 1.5 degrees of the M49 sub-cluster. The total sample includes 117 objects with morphological types between S0/a and Im and BCDs. Because of the low visibility of the Virgo cluster during the ISO mission and because of the low detection rate of small galaxies with ISOCAM, the 18 Im and BCDs in the cluster core could not be observed. The resulting sample is still unbiased but includes only 99 objects, with 26 spirals in the cluster core, and 73 spirals, irregulars and BCDs in the cluster periphery. The observed sample thus constitutes an optically-selected, volume-limited complete sample, ideal for statistical analyses. A few early-type galaxies were serendipitously observed in some of the fields. These do not constitute a complete sample in any sense, but because of their random selection, they can be used as an unbiased reference sample of early-type objects. Given the different densities of galaxies and of the intergalactic medium of the two selected regions, the observed sample can be used to study the effects of the environment on the dust properties of galaxies. However we show in Sect. 4.1 that the integrated Mid-IR fluxes of the spirals are not significantly affected by the environment, so that the present sample is a true reference sample.

## 3. Observations and data reduction

A complete description of the observations and data reduction will be presented in a forthcoming paper (Boselli et al., in preparation). The observations were part of the ISO Central Program: all galaxies were observed during one of the few visibility windows of the Virgo cluster during the ISO mission, in the summer of 1996. The  $32 \times 32$  pixel long-wavelength camera was used to make a raster map covering largely the galaxy, with a shift (then overlap) of 16 pixels between successive positions. The pixel size was  $6'' \times 6''$ .  $3 \times 3$  rasters were made for galaxies with the smallest angular dimensions, while larger rasters were adopted for giant or extended objects. The elementary integration time was 2 seconds, with 16 to 20 integrations per position. To minimize the effects of transients of the detector on the flux calibration of the source, 40 to 70 integrations per position were used in the first raster position every time the background was expected to change significantly from the previous target, thus for significantly different pointings and for different filters. In order to minimize the overhead time for galaxy pointing and for the stabilisation of the detector, galaxies were observed in a concatenated mode, with a complete sequence of observations of 5-10 nearby galaxies in a given (and fixed) filter. All galaxies were observed in 2 filters, LW2 ( $\lambda = 6.75 \mu\text{m}$ ,

$\Delta\lambda=5.00\text{--}8.50\ \mu\text{m}$ ) and LW3 ( $\lambda = 15.0\ \mu\text{m}$ ,  $\Delta\lambda=12.0\text{--}18.0\ \mu\text{m}$ ). Images were reduced following the standard CIA/IDL<sup>1</sup> procedures available at the ISOCAM center at the CEA in Saclay: images were dark-subtracted, flat-fielded, deglitched, corrected for the transient response of the detector, and combined. The total fluxes were determined using the IMCNTS routine in IRAF/Xray after subtraction of the sky background; counts were transformed in fluxes using the conversion factors given in the ISOCAM manual. The absolute fluxes are believed to be accurate to within 30%, mainly due to calibration errors, but the relative fluxes of the observed galaxies are certainly more accurate. The detection rate is 70% at 6.75  $\mu\text{m}$  and 55% at 15.0  $\mu\text{m}$  (see Table 1). Note that none of the Im galaxies have been detected. For undetected galaxies, an upper limit has been determined as:

$$F_{limit(\lambda)} = 2\sigma_\lambda(5 \times 5 \text{ pixels})(\text{mJy}) \quad (1)$$

where  $\sigma_\lambda$  is the background noise per pixel at a given  $\lambda$ . We thus assume that a galaxy has an extended emission ( $5 \times 5$  pixels, or  $30 \times 30$  arcseconds).

#### 4. The Mid-IR emission of galaxies

In this section we analyse the Mid-IR integrated properties of the observed galaxies by comparing the CAM observations to data at other wavelengths: Far-IR data at 60 and 100  $\mu\text{m}$  are taken from IRAS (Thuan & Sauvage 1992), near-IR magnitudes and optical data from Boselli et al. (1997b) and Boselli (in preparation), and UV data at 2000 Å from Deharveng et al. (1994), Donas et al. 1998 (in preparation) and references therein.

##### 4.1. Mid-IR luminosity distribution

Since the observed sample is complete, it can be used to determine the luminosity distribution of galaxies of different types in the Mid-IR. The poor statistics for early-types and the low detection rate for the dwarf irregulars (see Table 1), allow us to determine a reliable luminosity distribution only for spirals.

The Mid-IR luminosity distribution at 6.75 and 15  $\mu\text{m}$  is shown for different morphological classes in Fig. 1a and b. Sm and Amorphous galaxies are included in the spiral class, while the Sm/BCD and the Im/BCD are included in the BCD class. The Mid-IR luminosities have been computed as:

$$L_\nu = 4\pi D^2 F_\nu \delta_\nu \quad (2)$$

where  $\delta_\nu$  is the filter width; at 6.75 ( $\delta_{6.75\mu\text{m}} = 11.57 \cdot 10^{12}$  Hz) and 15  $\mu\text{m}$  ( $\delta_{15\mu\text{m}} = 5.04 \cdot 10^{12}$  Hz)  $L_\nu$  is given by:

$$L_{6.75\mu\text{m}} = 4\pi D^2 F_{6.75\mu\text{m}} 2.724 \times 10^2 L_\odot \quad (3)$$

<sup>1</sup> CAM Interactive Analysis, CIA, is a joint development by the ESA Astrophysics Division, and the ISOCAM Consortium led by the ISOCAM P.I., C. Cesarsky, Direction des Sciences de la Matière, CEA, France

**Table 1.** Statistics and detection rate for the observed galaxies

Type	<i>observed</i>	<i>detected</i>		<i>K'</i>
		6.75 $\mu\text{m}$	15 $\mu\text{m}$	
E*	1	1	1	1
S0*	2	2	2	2
S0/a	5	5	3	5
Sa	11	10	10	11
Sab	4	4	4	4
Sb	3	3	3	3
Sbc	1	1	1	1
Sc**	22	20	17	21
Scd	4	4	2	4
Sd-Pec-	6	4	3	6
Amorph.				
Sm	9	6	6	9
Im	21	0	0	10
BCD	9	5	3	6
Sm/BCD	2	2	2	2
Im/BCD	4	2	0	2

\*: serendipitously observed in the field of nearby selected galaxies \*\*: one of the 22 Sc galaxies (VCC 1018), serendipitously observed in the field of a nearby target, is not a cluster member and will not be used in the following analysis.

and

$$L_{15\mu\text{m}} = 4\pi D^2 F_{15\mu\text{m}} 1.184 \times 10^2 L_\odot \quad (4)$$

where  $D$  is the distance in Mpc (we adopt 17 Mpc for Virgo, as recently determined from Cepheid distances observed with the HST; see for a recent review van den Bergh, 1996), and  $F_{6.75\mu\text{m}}$  and  $F_{15\mu\text{m}}$  are the fluxes at 6.75 and 15  $\mu\text{m}$ , in mJy.

As shown by Sandage and collaborators (1985), the optical luminosity function of spiral, elliptical and S0 galaxies in the Virgo cluster ends at  $B_T = 16$  mag, while dwarfs reach lower magnitudes. Our sample being complete to  $B_T = 18$  mag, since includes all the Virgo spirals in the limited observed volume. 90 % and 82 % of the observed spirals (Sa-Sd-pec-Amorph.) are detected at 6.75 and 15  $\mu\text{m}$  respectively, the Mid-IR luminosity distribution shown in Fig. 1 can be taken as representative at least for the spiral population. Spiral, elliptical and S0 galaxies have Mid-IR luminosities ranging from some  $10^6$  to  $10^9$  solar luminosities both at 6.75 and 15  $\mu\text{m}$ , while dwarfs have Mid-IR luminosities generally lower than  $10^7 L_\odot$ . In order to compare galaxies of different size and mass we construct the normalized Mid-IR luminosity distribution by dividing the Mid-IR fluxes of the target galaxies by the flux in the near-IR  $K'$  band, which is a good indicator of the total mass of galaxies (Gavazzi et al. 1996, see Fig. 1a and b). The  $K'$  flux (in mJy) is defined as:

$$F_{K'}(\text{mJy}) = 0.63 \times 10^6 \times 10^{-K'_{\text{mag}}/2.5} \quad (5)$$

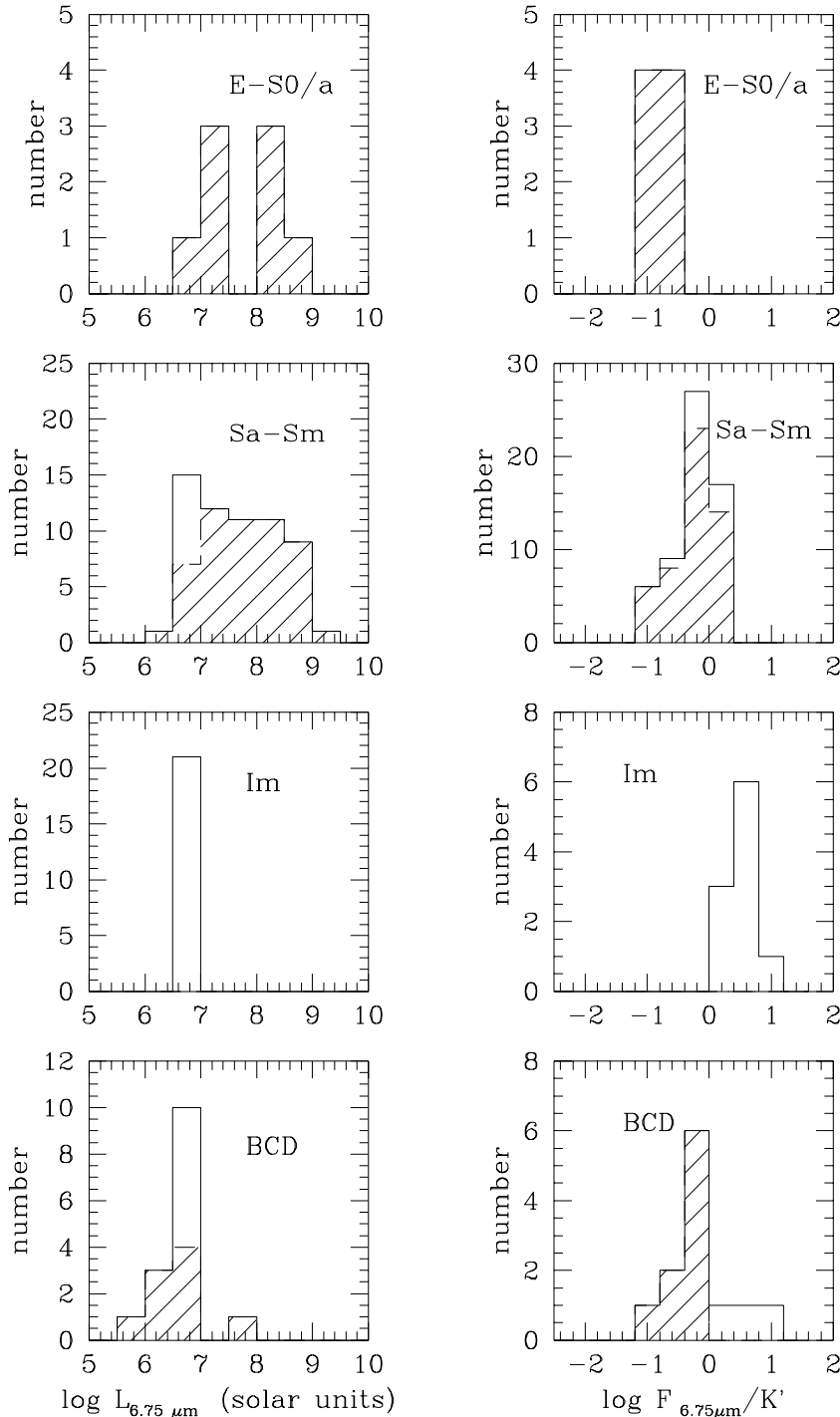


**Fig. 1.** The Mid-IR luminosity distribution at  $6.75 \mu\text{m}$  (left column) and the one normalized to the flux in the K' band (right column) for detected (dashed line, shaded histogram) and undetected (full line, empty histogram) galaxies of different morphological type. 11 Ims and 3 BCDs with no K' magnitudes are excluded from the normalized luminosity distribution.

where  $K'\text{mag}$  is the K' magnitude corrected for extinction. The K' magnitudes have been obtained by integrating along circular annuli the NICMOS 3 images of the target galaxies to the optical diameter at the  $25 \text{ mag arcsec}^{-2}$  isophote, as described in Boselli et al. (1997b). As for the Mid-IR data, the K' magnitudes are not extrapolated values; they represent the total emission of the galaxy. As

indicated in Table 1, this can be done for all the selected spirals and early-types, but K' magnitudes are not available for a few Ims and BCDs with  $B > 16.0$  (see Boselli et al. 1997b).

We checked the influence of the environment by comparing the luminosity distribution of galaxies in the cluster core to that of galaxies in the periphery. Since dwarf

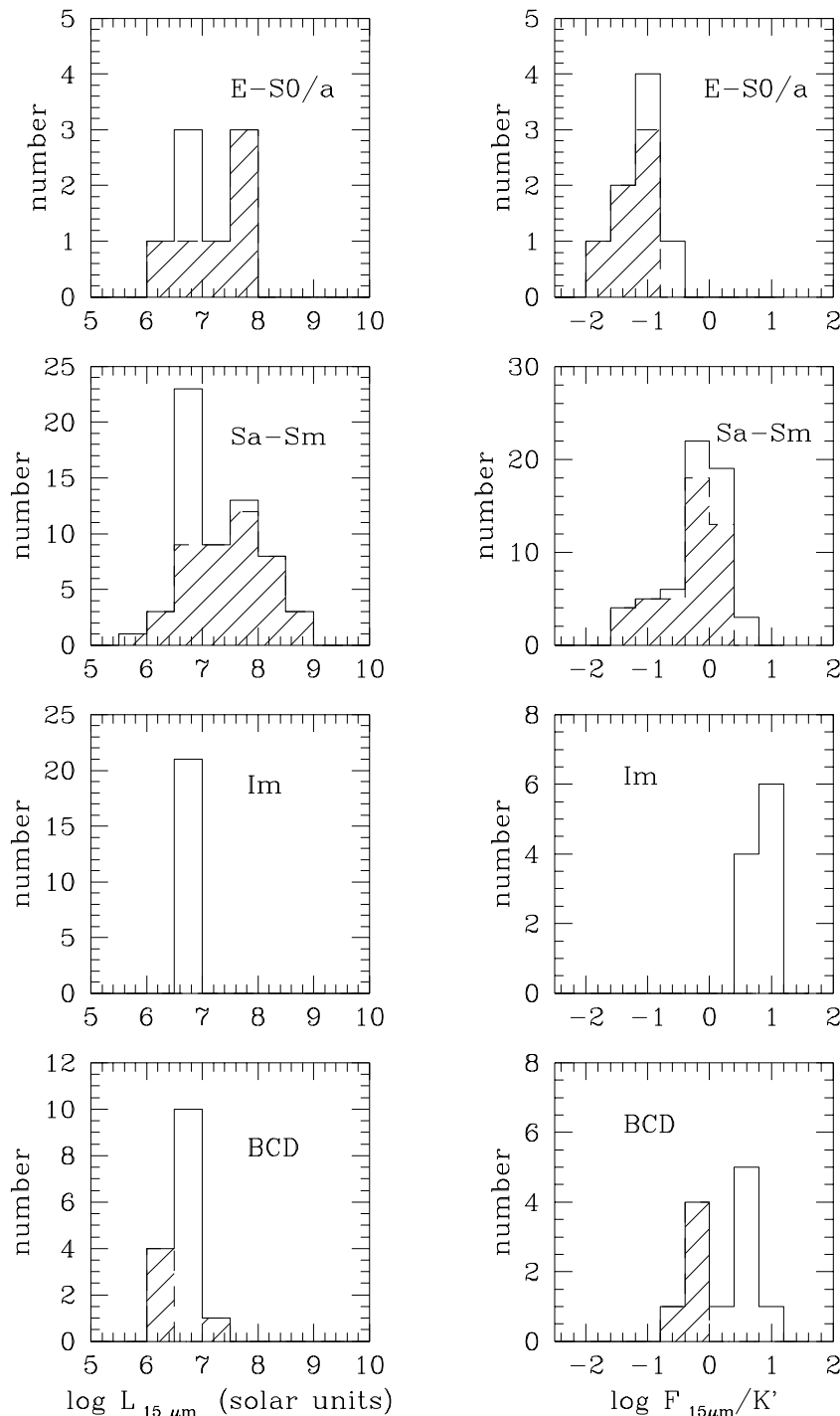


**Fig. 2.** The Mid-IR luminosity distribution at  $15.0\ \mu\text{m}$  (left column) and the one normalized to the flux in the K' band (right column) for detected (dashed line, shaded histogram) and undetected (full line, empty histogram) galaxies of different morphological type. 11 Ims and 3 BCDs with no K' magnitudes are excluded from the normalized luminosity distribution.

galaxies have been observed only in the periphery of the cluster (see Sect. 2), the present test was performed only for spirals (Sa-Sm). A survival analysis (Isobe et al. 1986), done to take into account upper limits, has shown, at least to the first order, no statistically significant differences between the normalized Mid-IR emission of spirals in the core and in the periphery of the cluster. This result

can be deduced by the inspection of Fig. 2, where the  $\log F_{6.75\mu m}/K'$  and  $\log F_{15.0\mu m}/K'$  are plotted versus the angular distance from the cluster centre (for type Sa-Sm). Galaxies in the core of the cluster have mean values of  $\log F_{6.75\mu m}/K' = -0.35 \pm 0.38$  and  $\log F_{15.0\mu m}/K' = -0.52 \pm 0.59$ , while galaxies in the periphery have  $\log F_{6.75\mu m}/K' = -0.22 \pm 0.37$  and  $\log F_{15.0\mu m}/K' = -0.27 \pm 0.50$ . The

results of the analysis on the effects of the environment on the Mid-IR emission of galaxies will be presented in a forthcoming paper (Boselli et al., in preparation).

To summarize, while the Mid-IR emission (per unit mass) of the spirals and later systems are comparable, the average 6.75 and 15  $\mu\text{m}$  to K' flux ratio of E, S0 and S0/a galaxies is significantly lower than that of spirals. At 15  $\mu\text{m}$ , where the difference is clearer, spirals have on average a Mid-IR emission per unit mass higher by more than one order of magnitude than E-S0/a. BCD galaxies have, on average, a Mid-IR emission per unit mass comparable to that of spirals. If Im galaxies had a Mid-IR emission per unit mass comparable to that of spirals, their low luminosities would make them undetectable by ISOCAM.

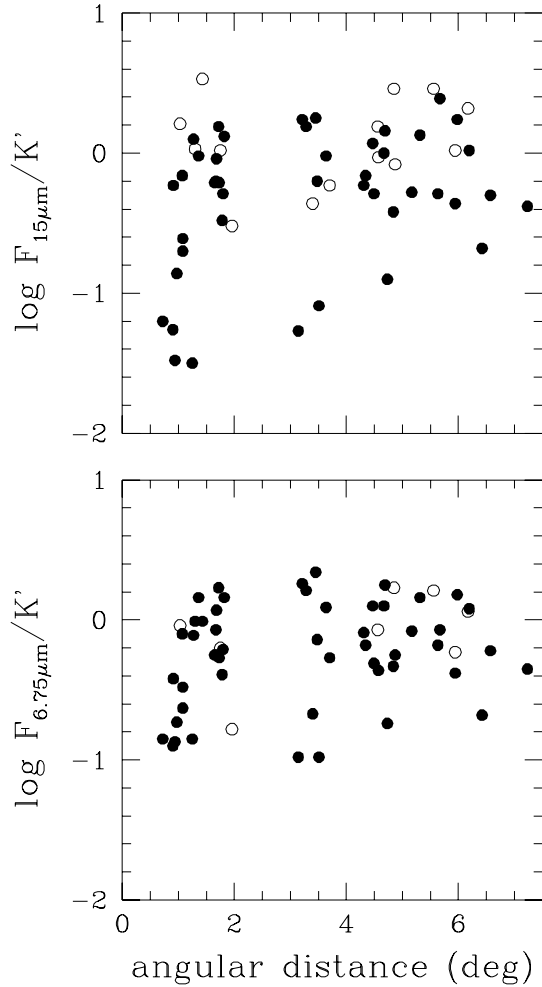


**Fig. 3.** The relationship between the  $\log F_{6.75\mu\text{m}}/K'$  (down) and  $\log F_{15.0\mu\text{m}}/K'$  (up) and the angular distance from the cluster centre for galaxies of type Sa-Sm. Galaxies in the core are all objects with an angular distance from the cluster centre  $\leq 2$  degrees. Empty dots are for undetected objects.

#### 4.2. The spectral energy distribution

We constructed the spectral energy distribution (SED) from the UV at 2000  $\text{\AA}$  to the Far-IR at 100  $\mu\text{m}$  for all the detected galaxies. They include, in order of increasing wavelength, UV data at 2000  $\text{\AA}$ , U (3650  $\text{\AA}$ ), B (4440  $\text{\AA}$ ), V (5500  $\text{\AA}$ ), J (1.25  $\mu\text{m}$ ), H (1.65  $\mu\text{m}$ ) and K' (2.10  $\mu\text{m}$ ) photometry, 6.75  $\mu\text{m}$  (ISOCAM), 12  $\mu\text{m}$  (IRAS), 15  $\mu\text{m}$  (ISOCAM), 60 and 100  $\mu\text{m}$  (IRAS) data. Optical and near-IR magnitudes are values integrated to the optical diameter at the 25 mag arcsec $^{-2}$  isophote, determined as described in Gavazzi & Boselli (1996).<sup>2</sup> Optical and near-IR data for spiral galaxies with type  $< \text{Sd}$  are corrected for galactic and internal extinction as described in Gavazzi & Boselli (1996). As shown by Buat & Xu (1996), the extinction for galaxies with type  $\geq \text{Sd}$  is  $\sim 0.2$  mag in the UV at 2000  $\text{\AA}$ , thus only  $\sim 0.1$  mag at optical wavelengths and even smaller in the near-IR. For this reason we prefer to not apply any internal extinction correction for Sd-Sm-Im and BCD galaxies.

Buat & Xu (1996) have shown that at 2000  $\text{\AA}$  the extinction is low ( $\sim 0.9$  mag), even in bright spirals; this is confirmed by the lack of relationship between the UV/K' flux ratio and the inclination of the sample galaxies, that we have checked. Because of the large uncertainty in the determination of the extinction in the UV, we prefer to adopt uncorrected values.

In order to compare the SED of galaxies with different luminosities, all fluxes are normalized to the near-IR K' flux and displayed in order of increasing morphological type (see Fig. 3). To estimate the contribution of the cold stellar component to the Mid-IR emission of the target galaxies, we plot for reference in Fig. 3 a black body at 3500 K adjusted on the peak of the emission of the cold stellar component, which is generally in the H band (dashed line).

As described in Gavazzi et al. (1996), the peak of the stellar emission is in the near-IR for massive, early-type spirals, while it moves to shorter wavelengths in late-type, low luminosity systems. The UV emission is only important in the latter objects (Gavazzi et al. 1996). The Mid-IR emission of early-type spirals can be partly due to the Rayleigh-Jeans tail of the cold stellar component at least at 6.75  $\mu\text{m}$ . The Far-IR emission of spirals and dwarfs seems correlated with the presence of young stars emitting in the UV. The Scds and the Sms have the highest Mid-IR emission per unit mass, while lower-luminosity Ims and BCDs, which are characterised by a stronger UV radiation field, have on average a 6.75 and 15  $\mu\text{m}$  emission comparable to that of Sc galaxies. In all spirals and dwarfs the flux density at 6.75  $\mu\text{m}$  is comparable to that at 15  $\mu\text{m}$ . In the few early-type objects (Ellipticals, S0

<sup>2</sup> For the few galaxies (5) with optical aperture or CCD photometry not available in the B band we used the photographic magnitudes from the Virgo Cluster Catalogue of Binggeli et al. (1985)

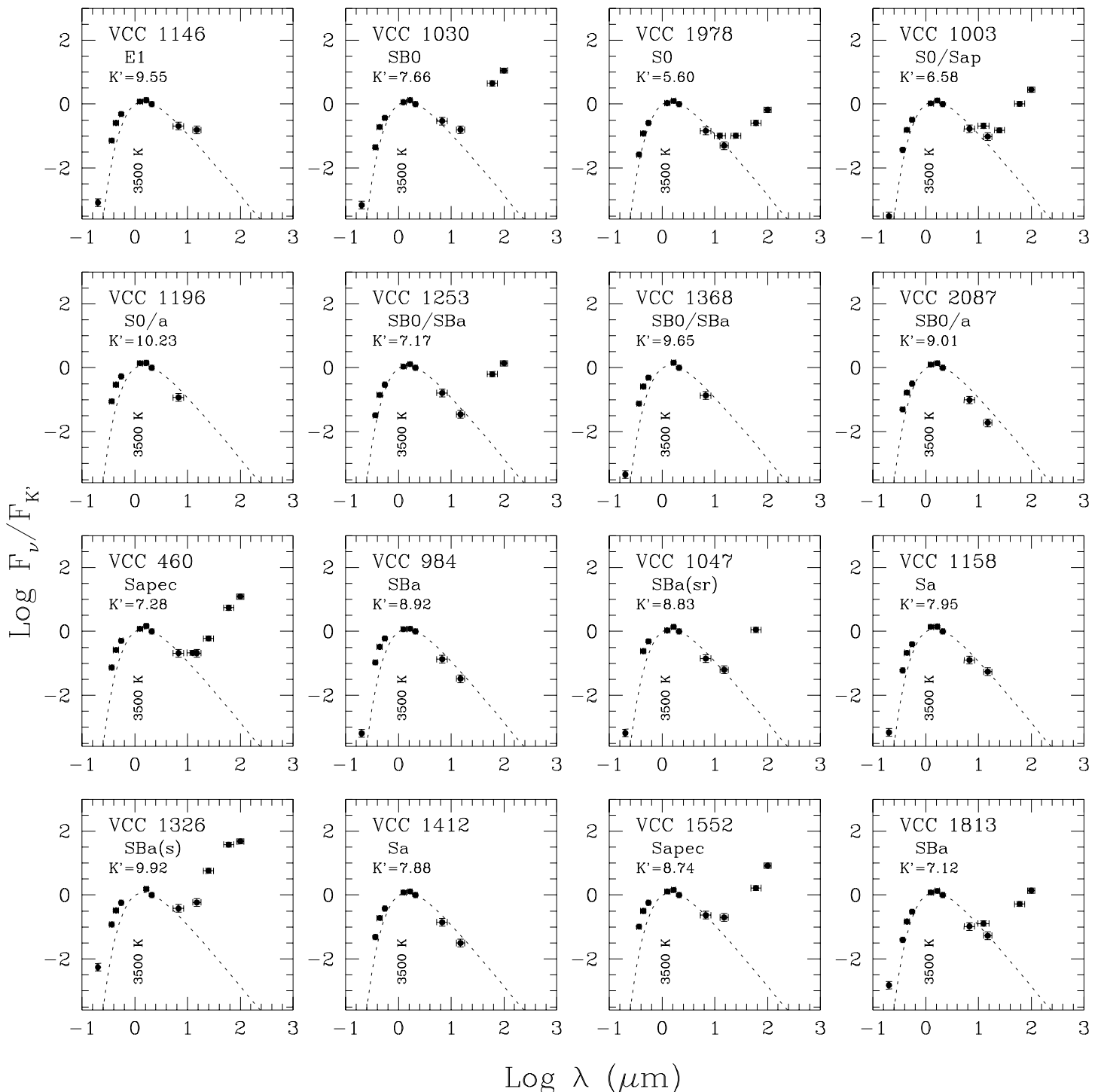


**Fig. 4.** The spectral energy distribution of the detected galaxies displayed in order of increasing morphological type. The dashed line indicates a black body at 3500 Kelvin. The VCC name and the morphological type is given for each galaxy.

and S0/a) the flux density at  $15 \mu\text{m}$  is significantly lower than that at  $6.75 \mu\text{m}$  and seems to follow the Rayleigh-Jeans tail of the cold stellar component. From this we conclude that the Mid-IR emission is dominated by the emission of the stars, as also shown by the analysis of the Mid-IR/Far-IR colour-colour relation (Boselli & Lequeux 1997; Madden et al. 1997).

In Table 2 we list the average values (in logarithmic scales) of the  $6.75 \mu\text{m}$  to  $K'$ ,  $15 \mu\text{m}$  to  $K'$  and  $6.75$  to  $15 \mu\text{m}$  flux ratios for the early-type objects in our sample.

The average value found for the early-type sample of Virgo galaxies listed in Table 2 is similar to that determined for the S0 VCC 1978 (NGC 4649), whose  $6.75 \mu\text{m}$  diffuse emission, contrary to spiral galaxies, is not associ-

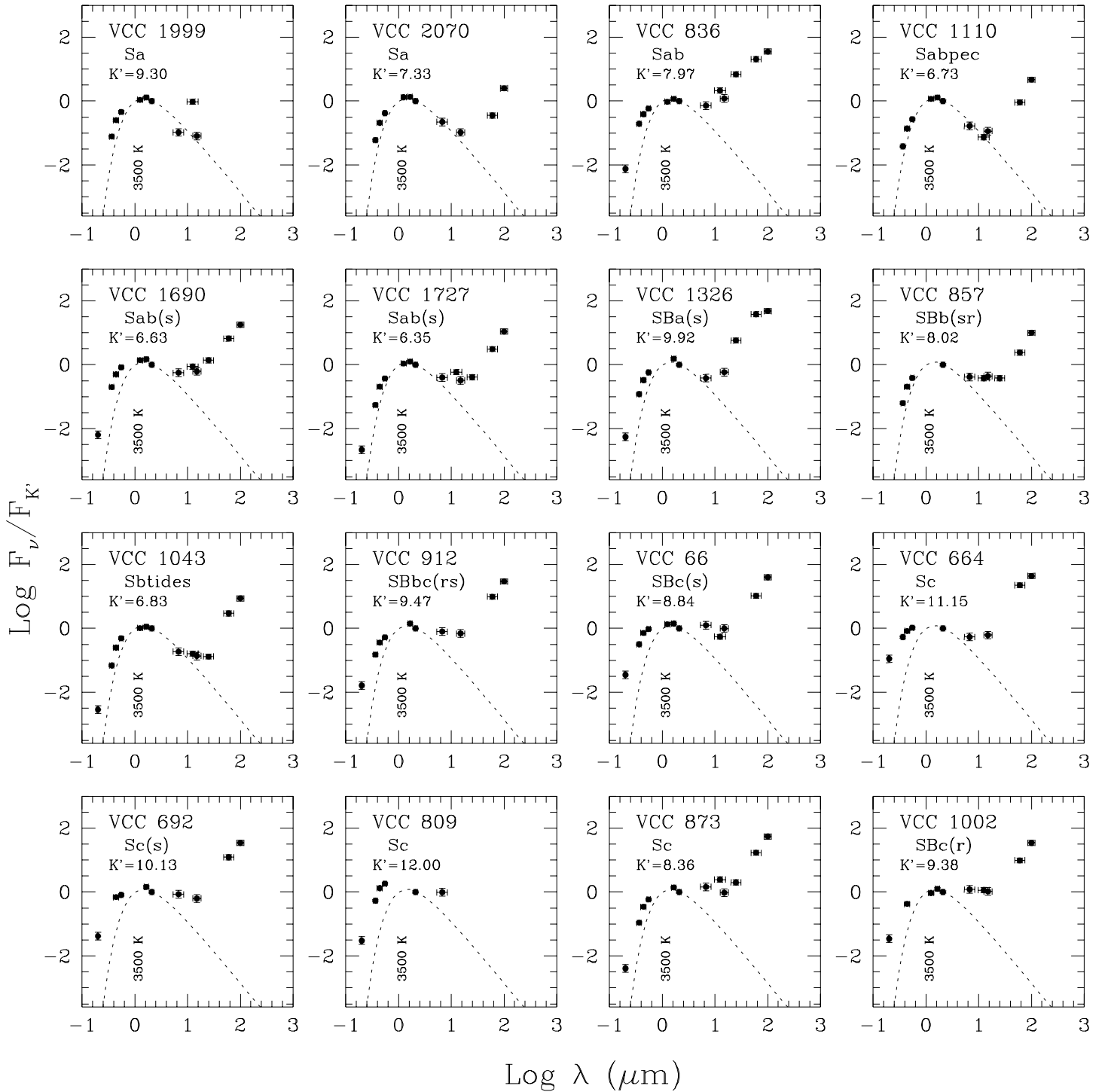


Fig. 5. Continued.

ated with any event of star formation as traced by the H $\alpha$  image, as shown by Boselli & Lequeux (1997). This observational evidence, along with the fact that most of the SEDs of the Mid-IR emission of the early-type galaxies in the present sample seem to follow the Rayleigh-Jeans tail of the cold stellar component at about 3500 K, suggests that the average value listed in Table 2 can be used, at least as a first approximation, to empirically estimate the

stellar contribution to the Mid-IR emission of later-type galaxies.

Boselli et al. (1997a) have shown that there is a clear correlation between the Far-IR emission and the UV flux of galaxies, while in the Mid-IR the 6.75 and 15  $\mu\text{m}$  normalized fluxes are proportional to the star formation rate only for low or moderate activities. Galaxies with strong UV radiation fields have, in general, a lower Mid-IR emis-



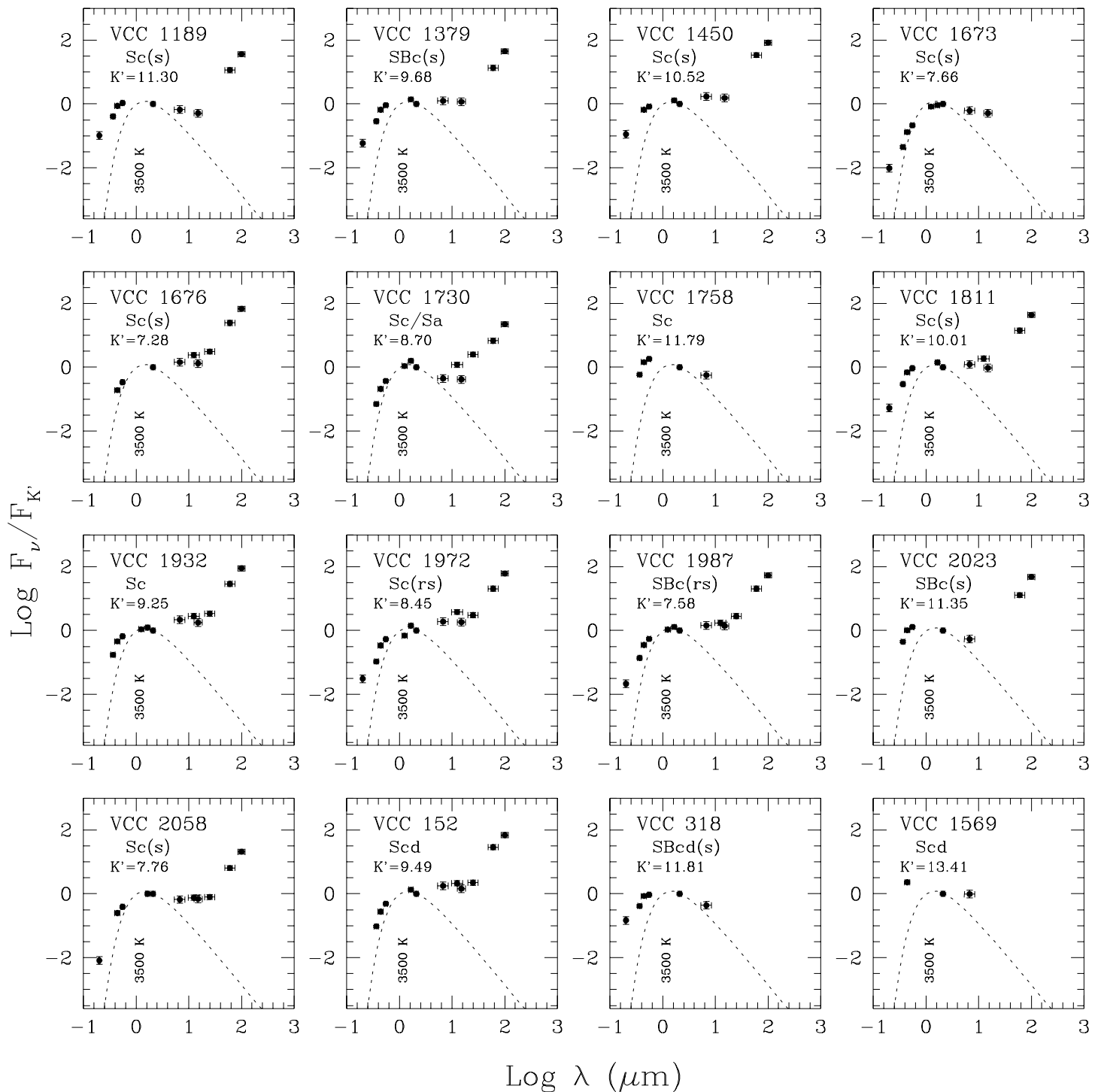


Fig. 6. Continued.

sion. This result can be seen in Fig. 4, where we plot the distribution of the spectral flux (a) and energy (b; defined as  $\nu F_\nu$  normalized to the energy in the  $K'$  band) for galaxies divided into 4 different classes of UV/ $K'$  flux ratios. Arbitrary thresholds on the UV/ $K'$  ratios are chosen to include in each group a similar number of objects. The difference between the UV to  $K'$  flux ratio of galaxies belonging to the 4 different classes is not the result of a se-

lection due to the internal extinction in the UV flux, since all galaxies are well mixed in inclination, but is real and reflects the properties of the UV radiation field in their ISM.

Black bodies with a temperature of  $T=20000$  K, 6000 K and 3500 K are fitted by eye to the UV, optical and near-IR data, while a modified ( $\lambda^{-2}$ ) black body with  $T=30$  K is fitted by eye to the cold dust component emitting

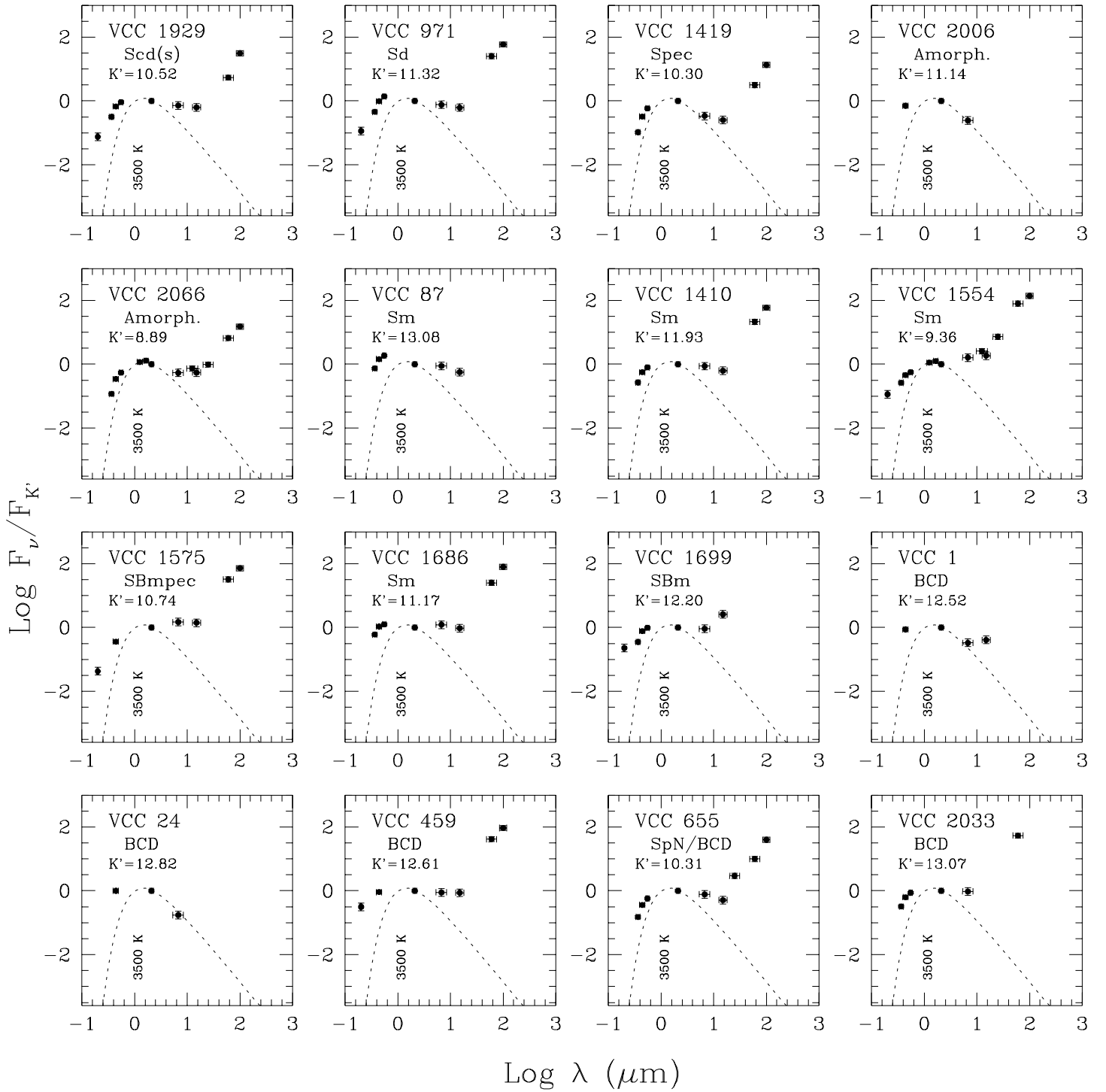


Fig. 7. Continued.

in the Far-IR. The stellar emission of galaxies with  $\log UV/K' < -2.8$  is dominated by the cold component peaked in the near-IR. A hot stellar component ( $T=20000$  K) is not needed to explain the UV emission of these galaxies, which is probably due to stars of intermediate mass and temperature. The cold stellar component ( $\lambda \sim 1 \mu\text{m}$ ) also dominates the peak of the energy distribution, with an energy balance  $\sim 100:1$  between the optical-near-IR and the

UV at  $2000 \text{ \AA}$ . A typical case is the S0/Sapec VCC 1003. The Mid-IR emission of these galaxies is dominated by the Rayleigh-Jeans tail of the cold stellar component at about  $3500$  K. As for galaxies with  $\log UV/K' < -2.8$ , the stellar emission and the energy distribution of galaxies with  $-2.8 < \log UV/K' < -2.0$  is dominated by the cold component peaked in the near-IR. A typical case is the Sab(s) VCC 1727. These galaxies are quiescent in the Mid-IR and in

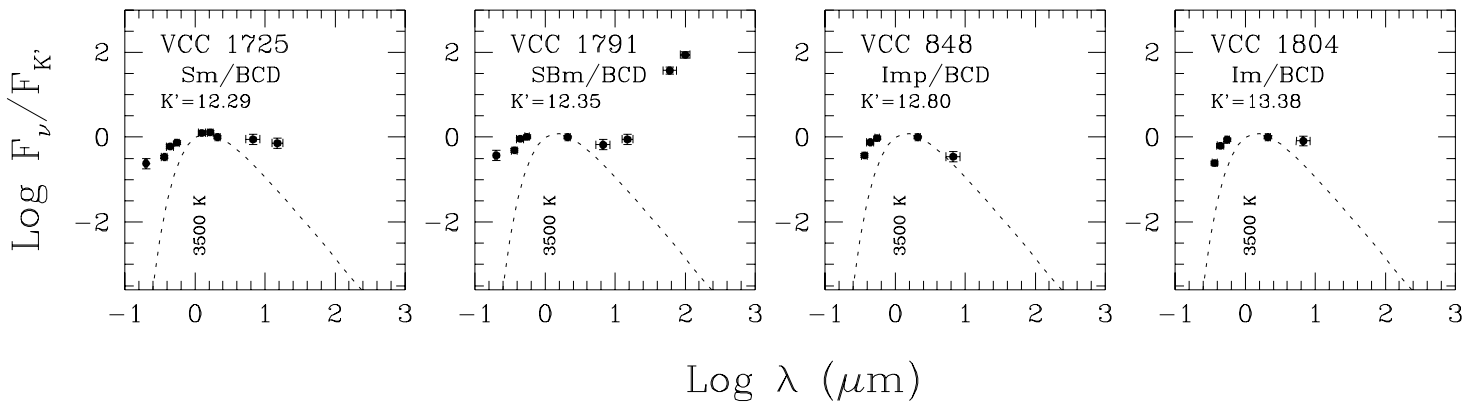


Fig. 8. Continued.

Table 2. Mid-IR to near-IR properties of the early-type galaxies of our sample; values are given in logarithmic scales

VCC	<i>NGC type</i>	$F_{6.75\mu\text{m}}/K'$	$F_{15\mu\text{m}}/K'$	$F_{6.75\mu\text{m}}/F_{15\mu\text{m}}$
1146	4458 <i>E1</i>	-0.69	-0.81	0.13
1030	4435 <i>SB0</i>	-0.53	-0.80	0.28
1978	4649 <i>S0</i>	-0.84	-1.30	0.46
1003	4429 <i>S0/Sap</i>	-0.77	-1.02	0.25
1196	4468 <i>S0/a</i>	-0.93	< -0.72	> -0.21
1253	4477 <i>SB0/SBa</i>	-0.79	-1.46	0.66
1368	4497 <i>SB0/SBa</i>	-0.87	< -0.98	> 0.11
2087	4733 <i>SB0/a</i>	-1.01	-1.72	0.71
average (detected galaxies only)		-0.80	-1.18	0.42
standard deviation:		0.15	0.37	0.22

the Far-IR if compared to the intermediate-class objects ( $-2.0 < \log \text{UV}/K' < -1.0$ ), which are also characterised by a higher contribution of the young stellar component to their global stellar emission (as for example VCC 1987). The galaxies with the most intense UV radiation fields ( $\log \text{UV}/K' > -1.0$ ), whose stellar emission and energy distribution are peaked at optical wavelengths, have the most intense Far-IR emission for the sample galaxies. However their Mid-IR emission is comparable to that of the objects with an intermediate star formation activity. A typical case is the BCD galaxy VCC 459. It is also interesting to mention that in some BCDs (VCC 1, VCC 24, VCC 848) the emission at  $6.75 \mu\text{m}$  follows the SED of a cold stellar component, while at  $15 \mu\text{m}$  the dust emission is important. However if the stellar emission of these galaxies is dominated by hot stars, a black body at  $3500 \text{ K}$  overestimates the stellar flux at  $6.75 \mu\text{m}$ , and there must be some dust emission at this wavelength.

To identify the heating sources of the dust emitting in the Mid- and Far-IR, we plot on Fig. 5 the relationships between the  $6.75$ ,  $15$  and  $100 \mu\text{m}$  fluxes normalized to the

$K'$  flux (first line) and to the UV flux (second line) versus the UV to  $K'$  flux ratio, which is widely used as a star formation tracer.

The strong relationship observed between the flux at  $100 \mu\text{m}$  and the UV flux confirms that the big grains responsible for the  $100 \mu\text{m}$  emission are heated by UV photons. The ratio of the energies emitted in the Far-IR and in the UV is strongly related to the UV flux, is close to unity in low-mass galaxies (open dots), and is  $\geq 10$  in high-mass, quiescent early-type spirals (filled dots). This strong relationship can be partly due to the effect of the extinction, which is expected to be higher in higher-mass, quiescent galaxies (Buat & Xu 1996), and in part to the fact that optical photons might significantly contribute to the heating of the dust grains in the quiescent sample. As shown by Boselli et al. (1997a), in low-mass galaxies with a strong star formation activity (open dots) the Mid-IR emission at  $6.75 \mu\text{m}$  and marginally at  $15 \mu\text{m}$ , is anticorrelated with the intensity of the UV radiation field, while the fluxes at  $6.75$  and  $15 \mu\text{m}$  are well correlated with the UV flux in massive spirals (filled dots).

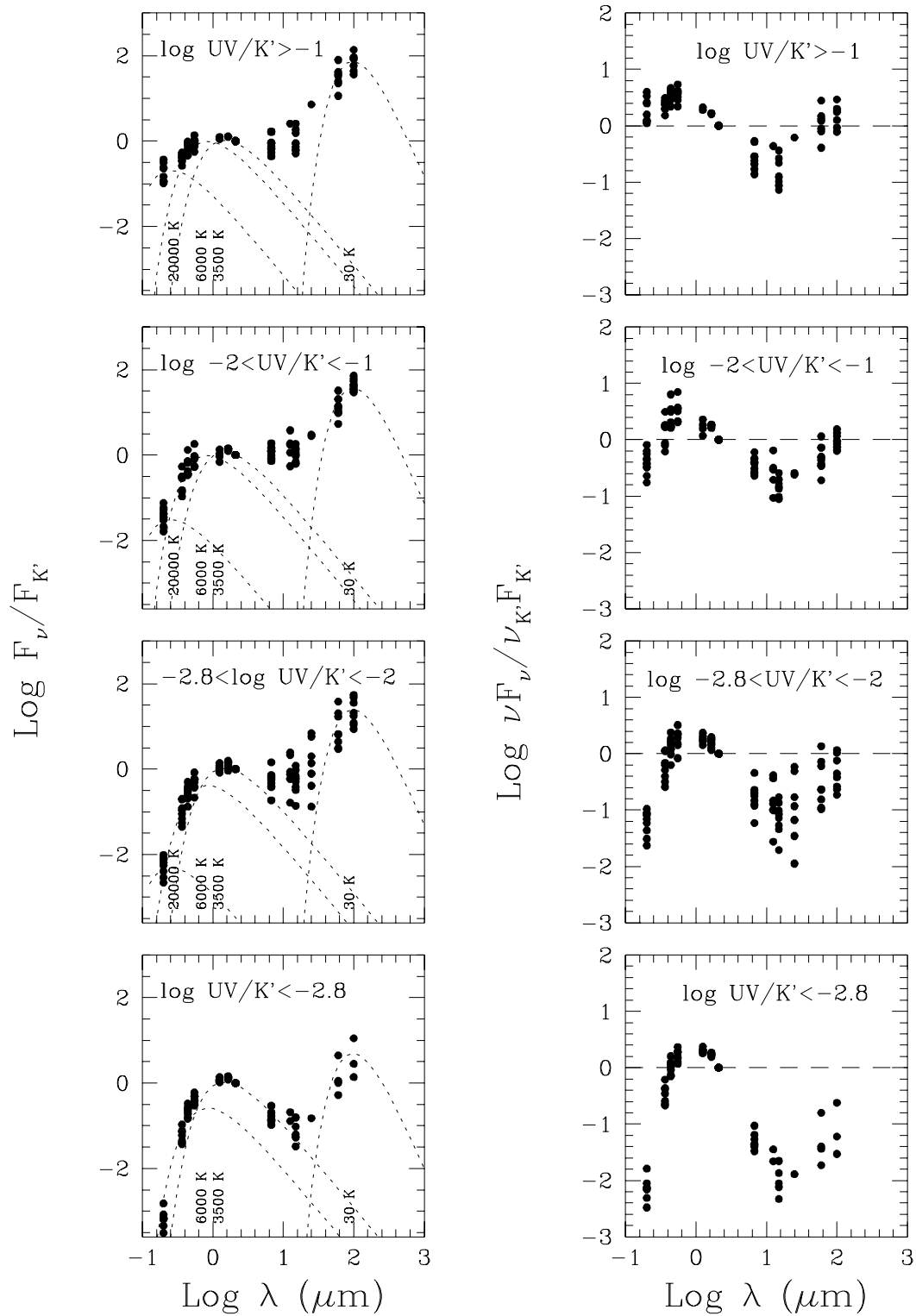


**Fig. 9.** The spectral energy distribution in fluxes (a) and in energy (b) defined as  $\nu F_\nu$  of the detected galaxies in 4 different classes of UV/K' flux ratios. The dashed line indicate black bodies at 20000, 6000 and 3500 degree Kelvin and a modified black body ( $\lambda^{-2}$ ) for the dust component at 30 K.

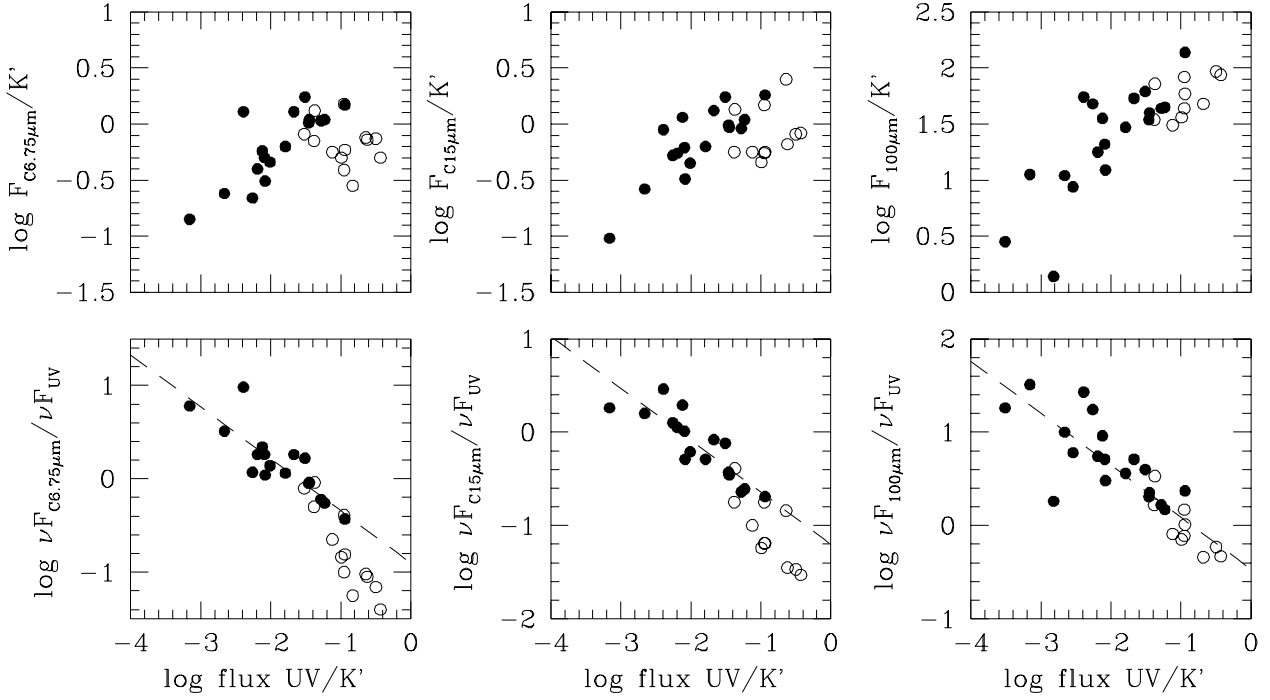


**Fig. 10.** First line: the relationship between  $\log F_{C6.75\mu m}/K'$ ,  $\log F_{C15.0\mu m}/K'$  and  $\log F_{100\mu m}/K'$  and the UV flux (normalized to the  $K'$  flux); second line: the relationship between  $\log \nu F_{C6.75\mu m}/\nu F_{UV}$ ,  $\log \nu F_{C15.0\mu m}/\nu F_{UV}$  and  $\log \nu F_{100\mu m}/\nu F_{UV}$  and the UV flux (normalized to the  $K'$  flux). The Mid-IR fluxes are corrected for the stellar contribution as described in Sect. 4.3. Open symbols indicate galaxies with  $K' > 10$  mag, filled dots are for objects with  $K' < 10$  mag. The dashed line is the best fit to the  $\log \nu F_{100\mu m}/\nu F_{UV}$  vs.  $\log UV/K'$  relationship, shifted in the  $\log \nu F_{C6.75\mu m}/\nu F_{UV}$  and  $\log \nu F_{C15.0\mu m}/\nu F_{UV}$  relationships to follow the data for bright galaxies (filled dots)

At the same time, the energy balance between UV photons and the Mid-IR emission does not hold in galaxies with an intense UV radiation field because these galaxies are relatively transparent to UV radiation. The Far-IR to UV energy ratio versus UV/ $K'$  relationship is shared in the Mid-IR only by massive spiral galaxies; in the dwarf population (open dots) the relationship between  $\nu F_{6.75\mu m}/\nu F_{UV}$ ,  $\nu F_{15.0\mu m}/\nu F_{UV}$  and the UV to  $K'$  flux ratio has steeper slopes, indicating that the relation between the incident UV photons and the emitting dust grains changes in strong UV radiation fields. The contribution of optical photons to the heating of the dust grains emitting in the Mid-IR is negligible because of their small physical dimensions, thus the Mid-IR to UV energy ratio vs. UV/ $K'$  relationships are probably entirely due to the extinction.

#### 4.3. Mid-IR and Far-IR dust emission of late-type galaxies

Using as template the small sample of early-type galaxies listed in Table 2, we can estimate and remove the average stellar contribution to the total Mid-IR emission of the

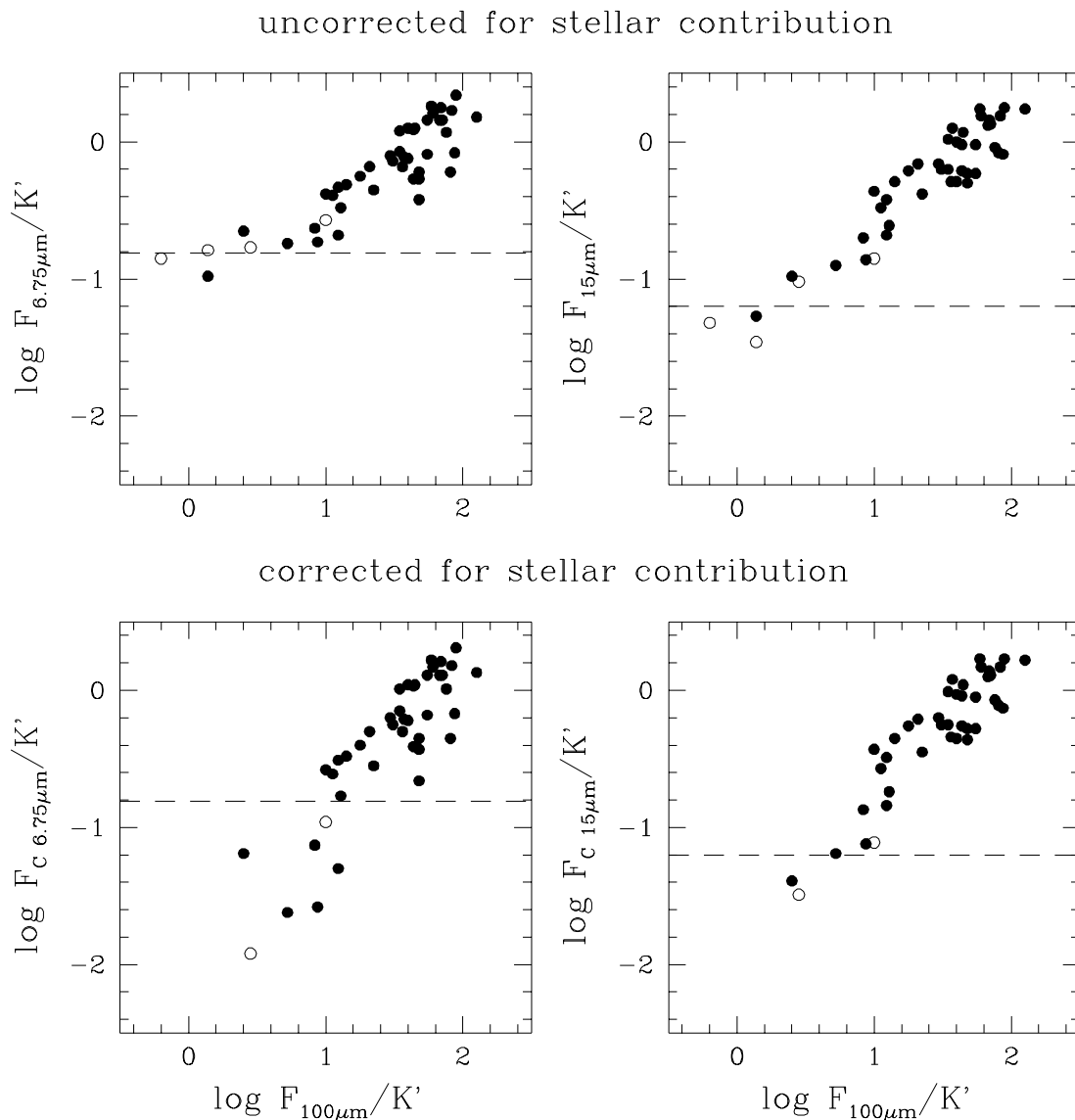
target galaxies. We thus obtain that the corrected fluxes at 6.75 and 15  $\mu m$  are given by the relations:

$$\text{Log} F_{C6.75\mu m}/K' = \text{Log}(F_{6.75\mu m}/K' - 0.158) \quad (6)$$

and

$$\text{Log} F_{C15.0\mu m}/K' = \text{Log}(F_{15.0\mu m}/K' - 0.063) \quad (7)$$

As shown in Fig. 6, when the corrected Mid-IR values are used, a relationship between the Mid-IR and the Far-IR emission is observed even at low dust emissions. Given the large uncertainty in the determination of the stellar contribution to the Mid-IR emission of early-type galaxies, this method is reliable only for objects whose emission at 6.75 and 15  $\mu m$  is dominated by dust, thus we exclude from the following analysis all objects with  $\log F_{6.75\mu m}/K' < -0.55$ . Corrected fluxes at 6.75 and 15  $\mu m$  are used throughout the following analyses. In Fig. 7 we plot the Mid- and Far-IR colours as function of the UV/ $K'$  flux ratio, the  $K'$  magnitude and the morphological type, coded as in Gavazzi & Boselli (1996): 3=Sa, 4=Sab, 5=Sb, 6=Sbc, 7=Sc, 8=Scd, 9=Sd, amorphous or peculiar, 10=Sm, 11=Im, 12=BCD, 13=Sm/BCD, 14=Im/BCD.



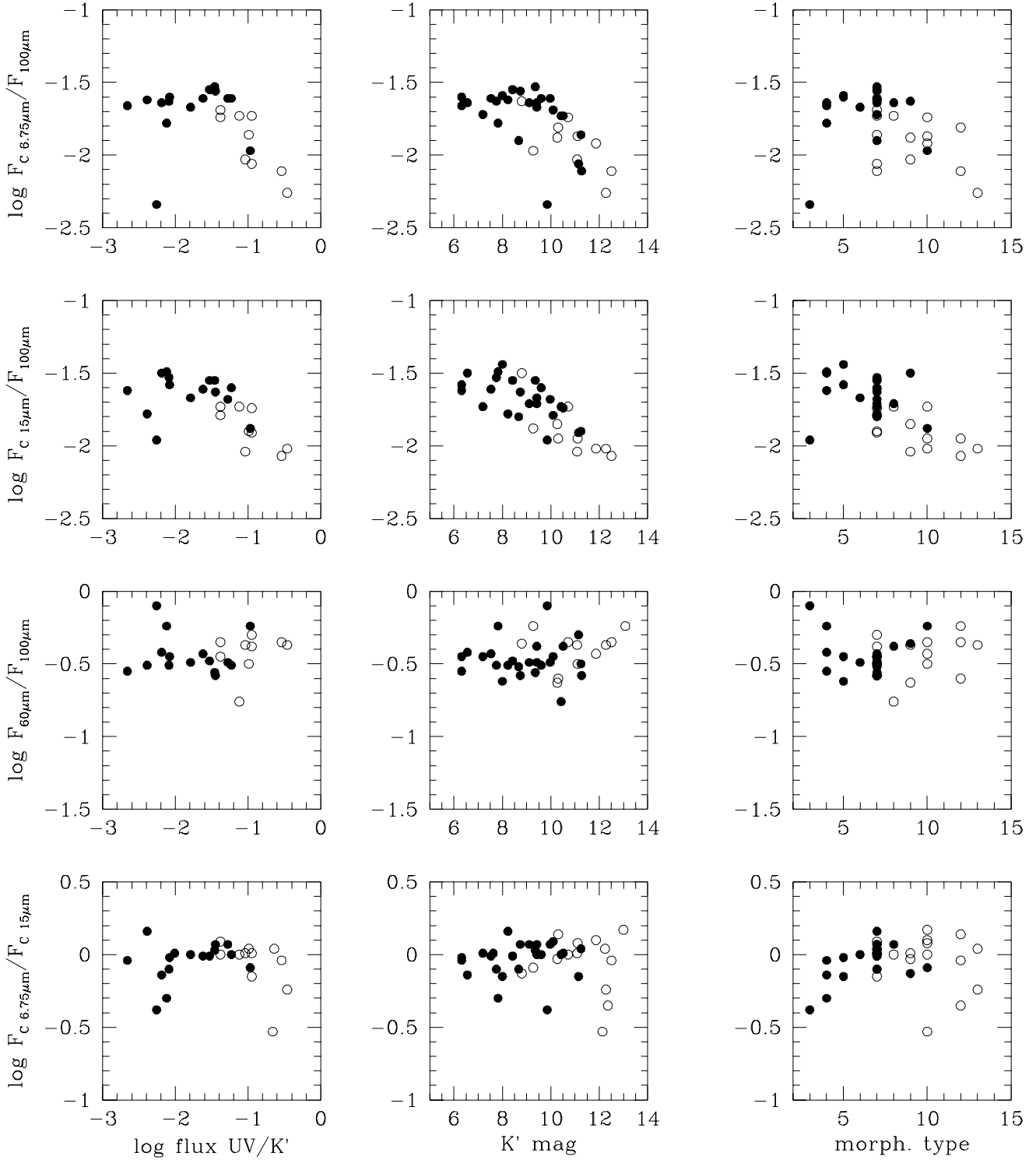
**Fig. 11.** The relationship between the normalized Far-IR emission at  $100\ \mu\text{m}$  and the Mid-IR  $6.75\ \mu\text{m}$  and  $15\ \mu\text{m}$  emission uncorrected (upper panels) and corrected (lower panels) for stellar contribution for the detected galaxies. Open symbols indicate early-type galaxies, filled symbols late-type objects. The dashed line indicate the average value found for early-type galaxies.

Figure 7 clearly shows that the dust properties in the Mid- and in the Far-IR are completely different in galaxies of different morphological type and/or mass or luminosity, characterised by a different UV interstellar radiation field. While the Far-IR  $F_{60\mu\text{m}}/F_{100\mu\text{m}}$  and Mid-IR  $F_{C6.75\mu\text{m}}/F_{C15\mu\text{m}}$  flux ratios are completely independent of the UV radiation field, the mass and the morphological type of the parent galaxy, the mixed  $F_{C6.75\mu\text{m}}/F_{100\mu\text{m}}$  and  $F_{C15\mu\text{m}}/F_{100\mu\text{m}}$  flux ratios are strongly anticorrelated with the UV radiation field, the  $K'$  luminosity and the morphological type.<sup>3</sup> First of all it must be noticed that

<sup>3</sup> The object with  $F_{C6.75\mu\text{m}}/F_{100\mu\text{m}} = -2.35$  and  $F_{C15\mu\text{m}}/F_{100\mu\text{m}}$  which does not follow the general trend in Fig. 7 is the Sa galaxy VCC 1326.

both the Far- and the Mid-IR colours  $F_{60\mu\text{m}}/F_{100\mu\text{m}}$  and  $F_{C6.75\mu\text{m}}/F_{C15\mu\text{m}}$  are quite similar in galaxies spanning a large range (more than 2 orders of magnitude) of star formation rates, and thus that at least for "normal", optically selected galaxies the infrared colours cannot be used as tracers of star formation. The same result has been obtained using other less direct star formation indicators such as the B-K' and U-B colours, and is valid for galaxies of all morphological types later than Sa, spanning a large range in absolute magnitude. This result seems in contrast with the general assumption that Far-IR colours are

The SED of this object shows that at least at  $6.75\ \mu\text{m}$  the Mid-IR flux can be strongly contaminated by stellar emission even if its  $\log F_{6.75\mu\text{m}}/K' > -0.55$ .



**Fig. 12.** The relationship between the Mid- and Far-IR colours  $F_{C6.75\mu m}/F_{100\mu m}$  (first line),  $F_{C15\mu m}/F_{100\mu m}$  (second line),  $F_{60\mu m}/F_{100\mu m}$  (third line) and  $F_{C6.75\mu m}/F_{C15\mu m}$  (fourth line) and the normalized UV flux (first column; open dots are galaxies with  $K'$  mag  $> 10$ , filled dots objects with  $K'$  mag  $< 10$ ), the  $K'$  magnitude (second column; open dots are galaxies with morphological type later than Scd, filled dots with morphological type earlier than Sd) and the morphological type coded as described in the text (third column; open dots are galaxies with  $K'$  mag  $> 10$ , filled dots objects with  $K'$  mag  $< 10$ ). The Mid-IR flux densities have been corrected for stellar contribution as described in the text; all galaxies have uncorrected  $\log F_{6.75\mu m}/K' > -0.55$ . The object with  $F_{C6.75\mu m}/F_{100\mu m} = -2.35$  and  $F_{C15\mu m}/F_{100\mu m}$  which does not follow the general trends is the Sa galaxy VCC 1326. The SED of this object shows that at least at  $6.75 \mu m$  the Mid-IR flux can be strongly contaminated by stellar emission.

good indicators of star formation (Helou 1986). It must be however noticed that most of the previous work was based on Far-IR selected samples which includes Far-IR bright galaxies such as starburst and active galaxies (Helou 1986), not included in the Virgo optically selected sample. Sauvage & Thuan (1994) have however shown that the 60 to 100  $\mu\text{m}$  flux ratio does not increase monotonically from E-S0 to late-type spirals and irregulars as expected from current dust models (e.g. Désert et al. 1990) if the Far-IR colour is simply related to the UV radiation field or to the star formation activity of the parent galaxy. Sauvage & Thuan (1994) interpreted this observational evidence as the result of the fact that, at least in galaxies of type E-S0 to Sbc, the Far-IR colours are mostly controlled by the spatial distribution of dust relative to stars, and not by the star formation activity as in later-type objects. Given the large intrinsic dispersion in the Far-IR colours in each morphological class, the present data do not exclude that the trend observed by Sauvage & Thuan (1994) is present.

As already shown by Boselli et al. (1997a), the mixed colours  $F_{C6.75\mu\text{m}}/F_{100\mu\text{m}}$  and  $F_{C15\mu\text{m}}/F_{100\mu\text{m}}$  are anticorrelated with the UV radiation field: galaxies with a strong star formation activity have in general a higher Far-IR to Mid-IR emission. Given the strong inverse relationship between the surface density of young ionizing stars and the luminosity or mass of a galaxy (Gavazzi et al. 1996), the strong anticorrelation between the flux ratios  $F_{C6.75\mu\text{m}}/F_{100\mu\text{m}}$  and  $F_{C15\mu\text{m}}/F_{100\mu\text{m}}$  and the UV flux can be translated into a well defined relationship between the flux ratios  $F_{C6.75\mu\text{m}}/F_{100\mu\text{m}}$  and  $F_{C15\mu\text{m}}/F_{100\mu\text{m}}$  and the mass of a galaxy. A relationship with a larger dispersion is also observed between the mixed Mid- to Far-IR colours and the morphological type. It is interesting to note that it is the near-IR luminosity more than the morphological type that discriminates the behaviour of the Mid- to Far-IR flux ratio of a given object, with luminous and massive galaxies characterized by a given  $F_{C6.75\mu\text{m}}/F_{100\mu\text{m}}$  and  $F_{C15\mu\text{m}}/F_{100\mu\text{m}}$  flux ratio and low mass objects with smaller Mid- to Far-IR flux ratios.

## 5. Discussion and conclusion

The availability of an unbiased, optically-selected and complete sample allows us to statistically draw the average Mid-IR properties of "normal" galaxies. We present for the first time the Mid-IR luminosity distribution at 6.75 and 15  $\mu\text{m}$  of a complete, optically-selected sample of late-type galaxies.

The present analysis clearly shows that the Mid-IR emission of ellipticals and lenticulars (morphological range E-S0/a) is dominated by the Rayleigh-Jeans tail of the photospheric emission of the cold stellar component emitting in the near-IR. This is still true for some early-type quiescent spirals. Figure 3 however does not exclude that some of these early-type objects have dust emitting in the

Mid-IR. Madden et al. (1997), by analysing a large sample of early-type galaxies observed with ISOCAM, have in fact shown that many objects characterized by the presence of atomic or molecular gas, or by nuclear star formation, have a Mid-IR emission already dominated by the dust at  $\lambda > 6 \mu\text{m}$  (Madden et al. (1997); Madden et al. in preparation).

In late-type galaxies the Mid-IR emission is generally dominated by dust. The strong relationship between the integrated UV flux at 2000 Å and the Mid-IR emission (both normalized to the mass of the galaxy) observed by Boselli et al. (1997a) indicates that the very small dust grains and the UIB carriers responsible for the emission at 6.75 and 15  $\mu\text{m}$  are heated preferentially by hot, massive stars. This is also confirmed by the good morphological correspondence between the peaks of the emission at 6.75 and 15  $\mu\text{m}$  and the  $\text{H}\alpha$  images of some nearby, bright well-resolved late-type galaxies (Sauvage et al. 1996, Boselli & Lequeux 1997). However these dust grains and UIB carriers can also be heated by the visible light of evolved stars if its radiation density is large, as shown for example by the fact that elliptical galaxies with little UV radiation or the bulge of M 31 also exhibit 6.75 and 15  $\mu\text{m}$  dust emission (Madden et al. in preparation; Cesarsky D. et al. in preparation; Uchida et al., 1997).

However in low-luminosity late-type galaxies Boselli et al. (1997a) have shown that the integrated Mid-IR emission does not follow the mean UV radiation field: the Mid-IR emission of these objects does not increase, and may even decrease for high Far-UV fluxes. Figure 7 also shows that for such objects the ratio of the Mid-IR flux to the Far-IR flux decreases at low K' luminosities or small total masses (and strong Far-UV radiation fields). All this points to a lack of very small grains and UIB carriers in low-luminosity late-type galaxies, both per unit mass of gas and relative to the big grains that are responsible for the Far-IR emission. There are two possible explanations for this trend.

One can be the effect of metallicity (Sauvage et al. 1990). One expects a lower dust/gas mass ratio for these galaxies since the grains are mostly made of heavy elements, but this does not necessarily imply a lower small grain/large grain ratio. However such a lower ratio could result from a second-order effect: the lower abundance of carbon with respect to oxygen (and probably to silicon) might lower the abundance of carbonaceous grains which are often believed to dominate the Mid-IR emission in our Galaxy, relative to that of silicate grains which are less efficient emitters (see e.g. Dwek et al. 1997). Then the overall Mid-IR emission will decrease with respect to the Far-IR one which is believed to be always dominated by silicates.

The other possible interpretation of the low Mid-IR/Far-IR emission ratio has been proposed by Boulanger et al. (1988) who suggested that in radiation fields larger than  $\sim 50$  times that in the solar neighborhood up to 80



% of the grains emitting in the Mid-IR can be destroyed by UV photons. Such a high radiation field exists in large fractions of the volume of the dwarf galaxies with  $K' > 10$  mag.

With the present data we cannot choose between these two interpretations, which in fact may hold simultaneously. A study of the ISO data base when available will probably allow to solve this problem.

*Acknowledgements.* We wish to thank V. Buat, A. Contursi, J.M. Deharveng and G. Gavazzi for interesting discussions during the preparation of this work. A.B. thanks H. Facques for his hospitality during his staying in Paris. We thank J. Donas for providing us unpublished UV data. We thank the referee, B.T. Soifer, for interesting comments and suggestions.

## References

- Binggeli B., Sandage A., Tammann G., 1985, AJ 90, 1681  
 Binggeli B., Popescu C., Tammann G., 1993, A&AS 98, 275  
 Boselli A., Lequeux J., 1997, in: "Extragalactic Astronomy in the Infrared", Editions Frontières, ed. T. Thuan and G. Mamon, p237  
 Boselli A., Tuffs R., Gavazzi G., Hippelein H., Pierini D., 1997b, A&AS, 121, 507  
 Boselli A., Lequeux J., Contursi A., et al, 1997a, A&A, 324, L13  
 Boulanger F., Beichman C., Désert F., et al., 1988, ApJ, 332, 328  
 Buat V., Xu C., 1996, A&A, 306, 61  
 Deharveng J.M., Sasseen T., Buat V., et al. 1994, A&A 289, 715  
 Désert F.-X., Boulanger F., Puget J.-L. 1990, A&A 237, 215  
 Dwek E., Arendt R., Fixsen D., et al., 1997, ApJ, 475, 565  
 Gavazzi G., Boselli A., 1996, Astrophys. Letters and Comm. 35, 1  
 Gavazzi G., Pierini D., Boselli A., 1996, A&A 312, 397  
 Helou G. 1986, ApJ 311, L33  
 Isobe T., Feigelson E.D., Nelson P.I., 1986, ApJ 306, 490  
 Madden S., Vigroux L., Sauvage M., 1997, in: "Extragalactic Astronomy in the Infrared", Editions Frontières, ed. T. Thuan and G. Mamon, p229  
 Sandage A., Binggeli B., Tammann G., 1985, AJ, 90, 1759  
 Sauvage M., Thuan T., Vigroux L., 1990, A&A, 237, 296  
 Sauvage M., Blommaert J., Boulanger F., et al., 1996, A&A, 315, L89  
 Sauvage M., Thuan T., 1994, ApJ 429, 153  
 Thuan T., Sauvage M., 1992, A&AS 92, 749  
 Uchida K., Sellgren K., Werner M., 1998, ApJ 493, L109  
 van den Bergh S., 1996, PASP, 108, 1091